This article has not been copyedited and formatted. The final version may differ from this version.
DMD Fast Forward. Published on October 7, 2009 as doi:10.1124/dmd.109.028449

DMD 28449

In vitro metabolism of haloperidol and sila-haloperidol - new metabolic pathways resulting from carbon/silicon exchange

Tove Johansson, Lars Weidolf, Friedrich Popp, Reinhold Tacke, Ulrik Jurva

Discovery DMPK, AstraZeneca R&D Mölndal, Sweden (T.J.), Department of Chemistry, Medicinal Chemistry, University of Gothenburg, Gothenburg, Sweden (T.J.), Clinical Pharmacology & DMPK, AstraZeneca R&D Mölndal, Sweden (L.W.), Institut für Anorganische Chemie, Universität Würzburg, Am Hubland, Würzburg, Germany (F.P., R.T.), Lead Generation, AstraZeneca R&D Mölndal, Sweden (U.J.)

Primary laboratory of origin: Discovery DMPK, AstraZeneca R&D, Mölndal, Sweden

Running title: In vitro metabolism of haloperidol and sila-haloperidol

Corresponding author: Tove Johansson, Discovery DMPK, AstraZeneca R&D Mölndal, SE-431 83 Mölndal, Sweden.

Tel.: +46 31 7065006

Fax: +46 31 7763867

Email: tove.e.johansson@astrazeneca.com

Number of text pages: 19

Tables: 4

Figures: 9

References: 35

Word counts:

Abstract: 236

Introduction: 750

Discussion: 1155

[1] Abbreviations used are:

m/z, mass-to-charge ratio; HLM, human liver microsome; RLM, rat liver microsome; CYP, cytochrome P450, UDPGA, uridine 5'-diphosphoglucuronic acid

Abstract

The neurotoxic side effects observed for the neuroleptic agent haloperidol have been associated with its pyridinium metabolite. Previously, a silicon analogue of haloperidol (sila-haloperidol) was synthesized, which contains a silicon atom instead of the carbon atom in the 4-position of the piperidine ring. In the present study, the phase I metabolism of sila-haloperidol and haloperidol was studied in rat and human liver microsomes. The phase II metabolism was studied in rat, dog and human hepatocytes and also in liver microsomes supplemented with uridine 5'-diphosphoglucuronic acid (UDPGA). A major metabolite of haloperidol, the pyridinium metabolite, was not formed in the microsomal incubations with sila-haloperidol. For sila-haloperidol, three metabolites originating from opening of the piperidine ring were observed, a mechanism that has not been observed for haloperidol. One of the significant phase II metabolites of haloperidol was the glucuronide of the hydroxy group bound to the piperidine ring. For sila-haloperidol, the analogous metabolite was not observed in the hepatocytes or in the liver microsomal incubations containing UDPGA. If silanol (SiOH) groups are not glucuronidated, introducing silanol groups in drug molecules could provide an opportunity to enhance the hydrophilicity without allowing for direct phase II metabolism. To provide further support for the observed differences in metabolic pathways between haloperidol and sila-haloperidol, the metabolism of another pair of C/Si analogues was studied, namely trifluperidol and sila-trifluperidol. These studies showed the same differences in metabolic pathways as between sila-haloperidol and haloperidol.

DMD Fast Forward. Published on October 7, 2009 as DOI: 10.1124/dmd.109.028449
This article has not been copyedited and formatted. The final version may differ from this version.

Introduction

Haloperidol was developed in the late 1950s and was found to be a potent neuroleptic agent (Janssen et al., 1959). Haloperidol is a dopamine (D_2) receptor antagonist and is still used in the treatment of schizophrenia, although it may cause severe extrapyramidal side effects including parkinsonism and tardive dyskinesia (Levinson, 1991; Casey, 1995). The pyridinium metabolite of haloperidol has been proposed to be the cause of these neurotoxic side effects, since it structurally resembles MPP^+, an inducer of Parkinson's-like symptoms (Subramanyam et al., 1991a; Dauer and Przedborski, 2003).

In the search for analogues of haloperidol, a silicon analogue (sila-haloperidol) was synthesized, where the quaternary R_3COH carbon atom in the piperidine ring was replaced by a silicon atom (R_3SiOH). The synthesis, the physicochemical and pharmacological properties of sila-haloperidol have been reported previously (Tacke et al., 2004a; Tacke et al., 2008). As a minor part of an extensive study of sila-haloperidol, including synthesis and pharmacological properties, three major phase I metabolites in human liver microsomes were tentatively identified. One of these metabolites were proposed to be formed via *N*-dealkylation and the other two by opening of the piperidine ring (Tacke et al., 2008). The present study will focus on a thorough investigation of both phase I and II metabolism of sila-haloperidol, in comparison with those of haloperidol.

The use of organosilicon chemistry in drug design has been reviewed previously (Tacke and Linoh, 1989; Bains and Tacke, 2003; Showell and Mills, 2003; Mills and Showell, 2004; Pooni and Showell, 2006; Gately and West, 2007). Carbon and silicon both are Group 14 elements and are similar in that they form four covalent bonds with many other elements. However, there are also striking differences. Silicon (1.17 Å) has a larger covalent radius than carbon (0.77 Å), resulting in the formation of longer bonds and, therefore, in an increase of the size of the sila-analogue and an increase of its

conformational flexibility. Also, in general, an increased lipophilicity is observed for silicon compounds compared to their corresponding carbon analogues. Silicon (1.74, Allred-Rochow) is less electronegative than carbon (2.50), leading to different polarizations of analogous carbon- and silicon-element bonds, manifested by, e.g., an increased acidity of silanols compared to the analogous carbinols. These and other sila-replacement effects may affect the chemical and physicochemical properties and may also alter the biological properties. For example, altered bond lengths and angles may change the molecule's interaction with a receptor and, hence, the pharmacological selectivity and/or potency. Replacing a carbon by a silicon atom may increase the potency of a compound if the carbinol serves as a hydrogen bond donor within the pharmacophore, because a silanol is a better hydrogen bond donor than the corresponding carbinol (Bains and Tacke, 2003; Showell and Mills, 2003; Mills and Showell, 2004; Pooni and Showell, 2006).

Recently, silicon switches of marketed drugs have been reviewed (Pooni and Showell, 2006). The term carbon/silicon switch, also called sila-substitution, is used when a silicon analogue of a known drug is synthesized where one carbon atom is replaced by a silicon atom, leaving the rest of the structure unchanged. Examples of silicon switches are (besides sila-haloperidol) sila-venlafaxine, sila-fexofenadine and disila-bexarotene, studied in different in vitro systems (Pooni and Showell, 2006).

Venlafaxine is an antidepressant that blocks the reuptake of serotonin and noradrenaline. Venlafaxine and its silicon analogue sila-venlafaxine displayed similar physicochemical properties but different pharmacological selectivity profiles (Daiss et al., 2006). Fexofenadine is a histaminic H_1 receptor antagonist, used in the treatment of allergies. The sila analogue of fexofenadine was synthesized in order to compare the pharmacological properties. Fexofenadine and sila-fexofenadine displayed similar receptor

profiles when tested against a panel of histamine receptors (Tacke et al., 2004b). Bexarotene is used in the treatment of cutaneous T-cell lymphoma and is an RXR-selective retinoid agonist. The disila analogue (twofold sila-substitution) was synthesized to test the hypothesis that introducing silicon in the drug molecule would change the molecular shape, lipophilicity and electrostatic potential in order to alter the pharmacodynamic profile. Disila-bexarotene was shown to be an equally potent RXR agonist as the carbon analogue (Daiss et al., 2005).

The aim of this study was to investigate the phase I and phase II metabolism of sila-haloperidol in comparison with that of haloperidol, in order to test the hypothesis that replacement of the quaternary R_3COH carbon atom of haloperidol by a silicon atom may potentially change the metabolic pathways, e.g., the pathway leading to the potential neurotoxic pyridinium metabolite (Tacke et al., 2004a). In addition, the aim was to provide a thorough metabolic investigation of a silicon containing compound studied in different *in vitro* systems.

In addition to the metabolism studies of haloperidol and sila-haloperidol, another pair of structurally related carbon/silicon analogues was investigated, namely trifluperidol and sila-trifluperidol. Structures of the test compounds used in this study are shown in Fig.1.

Methods

Chemicals. β-NADPH (reduced form tetrasodium salt), leucine enkephalin acetate hydrate, trifluperidol, William's E medium without phenol red, 5,5-diethyl-1,3-diphenyl-2-iminobarbituric acid, uridine 5'-diphosphoglucuronic acid (UDPGA) trisodium salt and water free dimethyl sulfoxide were puchased from Sigma-Aldrich (St. Louis, MO), Methanol was purchased from Rathburn Chemicals (Walkerburn, Scotland). Formic acid,

ammonium acetate and ammonia solution (25% in water) were purchased from Merck (Darmstadt, Germany). Acetonitrile and haloperidol were purchased from Thermo Fischer Scientific (Waltham, MA). Gibco HEPES buffer solution (1 M), Gibco 10xHBSS buffer solution and Gibco L-glutamine (200 mM) were purchased from Invitrogen (Carlsbad, CA). Percoll separating solution (1.124 g/ml) was purchased from VWR International (West Chester, PA). Brij-58 was purchased from Fluka Chemie AG (Buchs, Switzerland). All solvents were of analytical grade and the water used in the experiments was obtained from a water purification system (Elgastat Maxima, ELGA, Lane End, UK). Sila-haloperidol, sila-trifluperidol and a synthetic reference compound of the *N*-dealkylated metabolite of sila-haloperidol were synthesized as their hydrochlorides (Popp, 2008; Nguyen, 2009). Synthetic reference compounds of reduced haloperidol (the secondary alcohol), the pyridinium ion metabolite and *N*-oxide 1 of haloperidol were kindly donated by Prof. Neal Castagnoli Jr (Subramanyam et al., 1991b).

LC-MS method. The samples were analyzed by liquid chromatography (Waters ACQUITY UPLC, Milford, MA), on a Waters Acquity UPLC BEH (C18 2.1 x 50 mm, 1.7 μm) column, at a flow rate of 750 μL/min (the column temperature was set at 40°C). Mobile phase A consisted of 5% acetonitrile and 0.1% formic acid in water and mobile phase B was 100% acetonitrile. At the start of the gradient, the acetonitrile content was 1% and was linearly increased to 50% over a period of 5 minutes. The acetonitrile content was then increased to 90% within 0.01 minutes. This condition was held for 0.69 minutes, and finally the initial mobile phase composition was restored within 0.01 minutes. The UPLC system was coupled to a Waters Q-TOF Premier instrument equipped with an electrospray ionization source. Leucine-enkephalin was used as the lock mass (*m/z* 556.2771) for accurate mass calibration and introduced using the Lock Spray interface at 20 μL/min (500

DMD Fast Forward. Published on October 7, 2009 as DOI: 10.1124/dmd.109.028449
This article has not been copyedited and formatted. The final version may differ from this version.

pg/μL). Unless stated elsewhere, samples were diluted 1:2 in mobile phase A, and aliquots of 5 μl were injected into the LC-MS system. Full scan spectra were acquired in the positive ionization mode. For acquisition of MS/MS spectra, the injection volume was 20 μl, and generally a collision energy ramp (10-30 eV) was used. The software programs used to process the data were MassLynx (version 4.1) and MetaboLynx (Waters). The mass-to-charge ratios of all relevant ions in the MS mode were determined within 5 ppm from the exact mass of the proposed structure.

Liver microsomal incubations. Human liver microsomes (HLMs) were purchased from BD Biosciences (San Jose, CA). The rat liver microsomes (RLMs) were purchased from CellzDirect/Invitrogen (Carlsbad, CA). In addition to being characterised by the manufacturers, the enzyme activities of the microsomes were confirmed against a panel of common substrates and in-house compounds. The incubation mixtures, containing 1.0 mg/ml of liver microsomal protein and 10 μM of substrate in 0.1 M phosphate buffer (pH 7.4), were pre-incubated for 5 minutes at 37°C. The reaction was initiated by adding NADPH at a final concentration of 1 mM, and the reaction mixtures were incubated for 60 minutes at 37°C. Control incubations were conducted in the absence of NADPH and in the absence of substrate. The reactions were quenched with an equal volume of ice-cold acetonitrile. The samples were vortexed for 10 seconds and then centrifuged for 10 minutes at 4°C, 4000 rpm (~ 2750 *g*).

For the liver microsomal incubations with UDPGA, the incubation mixtures, containing 1.0 mg/ml of liver microsomal protein (HLM or RLM), 0.5 mg/ml of Brij-58 and 100 μM of substrate in 0.1 M phosphate buffer (pH 7.4), were pre-incubated for 5 minutes at 37°C. The reaction was initiated by adding UDPGA at a final concentration of 3 mM, and the reaction mixtures were incubated for 0 or 60 minutes at 37°C. The reactions were quenched with two parts ice-cold acetonitrile. The samples were vortexed for 10

seconds and then centrifuged for 20 minutes at 4°C, 4000 rpm (~ 2750 *g*). The supernatants were diluted 1:5 with water prior to analysis.

Hepatocyte incubations. Human (mixed male/female), dog (female) and rat (female) cryopreserved hepatocytes were purchased from Celsius In Vitro Technologies (Baltimore, MA). In addition to being characterised by the manufacturers, the enzyme activites of the hepatocytes were confirmed against a panel of common substrates and in-house substances. Metabolite profiling was conducted using pooled cryopreserved animal hepatocytes at a substrate concentration of 4 μM. Substrate stock solutions of 10 mM were prepared in dimethyl sulfoxide. The hepatocytes were quickly thawed in a water bath kept at 37°C and transferred to 50 ml falcon tubes containing prewarmed hepatocyte incubation media. The hepatocyte incubation media consisted of 2 mM L-glutamine, 25 mM HEPES, diluted with William's E medium to 500 ml, and the pH was set to 7.4. After centrifugation (100 *g* at 25°C for 6 minutes), the supernatant was removed and the pellet was resuspended in Percoll. After centrifugation (100 *g* at 25°C for 20 minutes) the pellet was resuspended in hepatocyte incubation media. The cells were counted using the trypan blue exclusion method. After dilution to a concentration of 2 million cells/ml in hepatocyte incubation media, the hepatocyte suspension was added to each well (25μl/well) of a 96-well plate. The plate was placed in the incubator (Galaxy R CO_2 Incubator) to pre-incubate for 10 minutes and the reaction was initiated by adding the pre-warmed substrate solution (25 μl of 8 μM substrate solution/well). Blanks without substrate were also prepared. For the time zero time-point, the hepatocyte incubations were first treated with the quenching solution prior to the addition of substrate solution. The incubations were stopped after 120 minutes by adding three volumes of ice-cold stop solution; acetonitrile containing 0.8 % formic acid and a volume marker (1 μM 5,5-diethyl-1,3-diphenyl-2-iminobarbituric acid).

The plates were kept at -20°C for at least 20 minutes, and then centrifuged at 2750 *g* at 4°C for 20 minutes. The supernatants were diluted 1:1 with water, and the plates were kept at -20°C until analysis.

Metabolite nomenclature. This is a metabolism study of four different compounds, and the intention was to highlight the similarities in the metabolic pathways of these test compounds, as well as the differences. Thus, we have chosen a metabolite nomenclature system that describes the metabolic pathways from which the metabolites originate. In cases where more than one metabolite originates from the same metabolic pathway, the metabolites are named based on their retention times, e.g., OH1 elutes before OH2.

Results

In the present study, the phase I and II metabolism of haloperidol were examined in order to compare the metabolic pathways with those of sila-haloperidol. Relative metabolite amounts of the fraction metabolized of haloperidol, estimated from integration of extracted ion chromatograms, are shown in Table 1. The cross-species metabolite scheme obtained from microsomal and hepatocyte incubations of haloperidol is shown in Fig. 2. The pyridinium metabolite was identified as a major metabolite in the microsomal incubations. Other metabolites formed were tentatively assigned as two separate hydroxylated products (OH1 and OH2), two diasteromeric *N*-oxides (*N*-oxide1 and *N*-oxide2), reduced haloperidol (Red) and an *N*-dealkylated metabolite (*N*-dealk). The pyridinium ion metabolite, reduced haloperidol and the first eluting *N*-oxide diastereomer (*N*-oxide1) were identified using synthetic reference compounds.

The major metabolites in hepatocytes were tentatively assigned to be reduced haloperidol, the *N*-dealkylated metabolite, the pyridinium metabolite and a direct glucuronidation metabolite (Gluc). The direct glucuronidation metabolite (glucuronidation of hydroxy group bound to the piperidine ring) was formed by rat and human hepatocytes but was not observed in dog hepatocytes. In humans the direct glucuronidation metabolite of haloperidol has been shown to be a major metabolite (Oida et al., 1989; Someya et al., 1992) and direct glucuronidation is also a major metabolic pathway in rats (Miyazaki et al., 1986). Minor metabolites in the hepatocytes were tentatively assigned as hydroxylations, *N*-oxides and another, earlier eluting, glucuronidation metabolite (+OH+Gluc). No product ion spectrum of this latter metabolite was obtained but since the mass corresponds to a hydroxylation and a glucuronidation, these reactions may occur in the same or two separate positions of the molecule. Also in the hepatocyte incubations, the pyridinium ion metabolite, reduced haloperidol and the first eluting *N*-oxide diastereomer (*N*-oxide1) were identified using the synthetic reference compounds.

The reduction of the carbonyl function of haloperidol to a secondary alcohol was observed in rat, dog and human hepatocytes. The reduction was also observed in rat and human liver microsomes but to a much smaller extent. Carbonyl reduction in liver microsomes has been reported previously (Beulz-Riche et al., 2001). It should be noted that estimation of the amounts of reduced metabolites formed in liver microsomes may be difficult because the metabolites may be subject to redox cycling.

Incubations with rat and human liver microsomes containing UDPGA, the cofactor necessary for glucuronidation, were performed. The direct glucuronidation metabolite of haloperidol was observed also in these incubations. Extracted ion chromatograms of the direct glucuronidation metabolites from the liver microsomal incubations with UDPGA are included in the Supplemental data.

Since haloperidol and its major metabolites are well characterized, by mass spectrometry and synthetic standard compounds (Fang et al., 1992; Gorrod and Fang, 1993; Narayanan et al., 2004), product ion spectra were not included in the Supplemental data.

Relative quantities of formed metabolites and remaining sila-haloperidol in microsomal and hepatocyte incubations, estimated from integration of extracted ion chromatograms, are summarized in Table 2. The cross-species metabolite scheme obtained from microsomal and hepatocyte incubations of sila-haloperidol is shown in Fig. 3. The product ion spectra and proposed fragmentation pathways of sila-haloperidol metabolites are shown in the Supplemental data.

The metabolism of sila-haloperidol in RLMs and HLMs differs from that of haloperidol. No sila-pyridinium metabolite was formed in the liver microsomes for sila-haloperidol. Instead, two ring-opened metabolites with $[M+H]^+$ ions at *m/z* 364 and *m/z* 382, respectively, were formed (Ring-opened1 and Ring-opened2). These two metabolites were the major metabolites in the HLMs, whereas other metabolites were tentatively assigned to be the *N*-dealkylated metabolite (*N*-dealk), hydroxylation product of Ring-opened1 (Ring-opened1+OH), reduced sila-haloperidol (Red) and a hydroxylated metabolite (OH). In the RLMs, the hydroxylated and the *N*-dealkylated metabolites were the major metabolites, while minor metabolites were tentatively assigned as reduced sila-haloperidol, the two ring-opened metabolites and the hydroxylation product of Ring-opened1. The structure of the *N*-dealkylated metabolite of sila-haloperidol was confirmed by comparing the retention time and the product ion spectrum with those of the synthetic reference compound while the proposed structures for the other metabolites of sila-haloperidol are tentative assignments based on interpretation of product ion spectra.

DMD Fast Forward. Published on October 7, 2009 as DOI: 10.1124/dmd.109.028449
This article has not been copyedited and formatted. The final version may differ from this version.

The fragment ions of sila-haloperidol and its metabolites are shown in Table 3. The product ion spectrum of sila-haloperidol, shown in Fig. 4, revealed three major fragment ions at *m/z* 165, *m/z* 164 and *m/z* 123. These three fragment ions all originate from the left hand side of the molecule and include the fluorophenyl group as shown by the proposed fragmentation pathways in Fig. 5. The proposed fragments for sila-haloperidol were used for tentative identification of the metabolites of sila-haloperidol. For example, an addition of 16 Da to the fragment at *m/z* 123 in the product ion spectrum of a metabolite indicates a hydroxylation on the fluorophenyl moiety. Following the same line of reasoning, the presence of the fragment at *m/z* 165 indicates that the left hand side of the molecule is intact and that the modification has occurred somewhere in the remaining part of the molecule.

One metabolite (OH) with a $[M+H]^+$ ion at *m/z* 408, corresponding to an addition of 16 Da to sila-haloperidol, was observed in the incubations with RLMs, HLMs and rat hepatocytes. As this metabolite eluted earlier than sila-haloperidol in the chromatogram, it was tentatively assigned as a hydroxylated rather than an *N*-oxygenated metabolite. The pK_a of the protonated amine is significantly higher than that of the corresponding *N*-oxide. Thus, under the acidic conditions used, the *N*-oxide is assumed to behave as being more lipophilic, whereas the hydroxylated metabolite would be expected to behave as more polar than the parent compound, based on their chromatographic retention times. Based on the product ion spectrum (shown in the Supplemental data), it is proposed that the hydroxylation occurs on the chlorophenyl ring of sila-haloperidol. The presence of the fragments at *m/z* 165, *m/z* 164 and *m/z* 123 in the product ion spectrum indicates that the left hand side of the molecule is unchanged. A hydroxylation on the piperidine ring would most likely give a major fragment corresponding to the loss of water in the product ion

spectrum (Ramanathan et al., 2000). The absence of such a fragment suggests the chlorophenyl moiety of sila-haloperidol as the most likely site for the hydroxylation.

The first eluting ring-opened metabolite gave a $[M+H]^+$ ion at *m/z* 364 and behaved as being more polar than the parent compound and the ring-opened metabolite2, based on their chromatographic retention times as shown in Table 2. The product ion spectrum of the ring-opened metabolite1, shown in Fig. 6, revealed two major fragment ions at *m/z* 172 and *m/z* 164. The proposed fragmentation pathways of this metabolite are shown in Fig. 7. A neutral loss of chlorophenyl vinyl silanediol (200 Da) from *m/z* 364 is proposed to give the fragment ion at *m/z* 164, which is also a major fragment ion in the product ion spectrum of sila-haloperidol. A neutral loss of fluorophenyl dihydropyrrole (163 Da) and ethene (28 Da) from *m/z* 364 is proposed to give the fragment ion at *m/z* 172, retaining the chlorine atom. The absence of the fragment ions at *m/z* 165 and *m/z* 123 implies that the carbonyl group is not present in the metabolite.

The second eluting ring-opened metabolite with a $[M+H]^+$ ion at *m/z* 382 behaved as being more polar than the parent compound and less polar than the ring-opened metabolite1, based on their chromatographic retention times as shown in Table 2. The proposed structure of the ring-opened metabolite2 is given in Fig. 3. The product ion spectrum is given in the Supplemental data along with a proposed fragmentation pathway.

The metabolite with a $[M+H]^+$ ion at *m/z* 380 (Ring-opened1+OH) corresponds to an addition of 16 Da to the ring-opened metabolite1. In the product ion spectrum, the fragment ion at *m/z* 172 was replaced by a fragment ion at *m/z* 188. Consequently, this metabolite was tentatively assigned as being hydroxylated on the chlorophenyl substituent (Fig. 3).

Sila-haloperidol was also incubated with rat, dog and human hepatocytes. Reduced sila-haloperidol was the major metabolite in the dog and human hepatocytes, while the *N*-

DMD Fast Forward. Published on October 7, 2009 as DOI: 10.1124/dmd.109.028449
This article has not been copyedited and formatted. The final version may differ from this version.

dealkylated metabolite and a metabolite originating from hydroxylation and glucuronidation (+OH+Gluc) were the major metabolites in rat hepatocytes.

Two metabolites, with $[M+H]^+$ ions at *m/z* 488 and *m/z* 584, respectively, appeared in the rat hepatocyte incubations but not in dog and human hepatocyte incubations. The metabolite with a $[M+H]^+$ ion at *m/z* 488 corresponds to an addition of 96 Da to sila-haloperidol, corresponding to a hydroxylation and a sulfate conjugation (+OH+Sulfate). The product ion spectrum displayed an initial loss of 80 Da to form the fragment ion at *m/z* 408. Since no loss of water is seen from the fragment at *m/z* 408, the hydroxylation is not likely occurring on an aliphatic carbon atom. Since the fragments at *m/z* 165 and *m/z* 123 are retained, the left hand side of the molecule is unchanged. Hence, the most likely route of formation for this metabolite is hydroxylation on the chlorophenyl moiety followed by a sulfate conjugation of that hydroxyl group, as proposed in Fig. 3.

The metabolite with a $[M+H]^+$ ion at *m/z* 584 corresponds to an addition of 192 Da to sila-haloperidol, corresponding to a hydroxylation and glucuronide conjugation. Except for an initial neutral loss of 176 Da instead of 80 Da, the product ion spectrum of *m/z* 584 is very similar to that of *m/z* 488 (+OH+Sulfate). Hence, the most likely route of formation for this metabolite is hydroxylation on the chlorophenyl moiety followed by a glucuronide conjugation of that hydroxyl group, as proposed in Fig. 3.

Noteworthy is that the hydroxylated metabolite of sila-haloperidol was the major metabolite in the RLMs while it was a minor metabolite in the rat hepatocytes, as illustrated in Table 2. Presumably, this metabolite was further metabolized by glucuronide conjugation and also sulfate conjugation. Any metabolite resulting from a direct glucuronidation of the SiOH group was not observed for sila-haloperidol. In the incubations with activated RLMs and HLMs supplemented with UDPGA, no direct glucuronidation of the SiOH group of sila-haloperidol was observed.

The identified metabolites were well separated using the liquid chromatographic method developed for these studies. Extracted ion chromatograms of the metabolites of haloperidol and sila-haloperidol, following incubation with human hepatocytes, are shown in Fig. 8. Sila-haloperidol is more lipophilic than haloperidol, and this is manifested by a shift in retention times of approximately 0.2 min. *N*-dealkylation and reduction occurs for both analogues in human hepatocytes. The differences in metabolism of the piperidine ring are obvious; haloperidol was metabolized to the pyridinium metabolite, and sila-haloperidol formed the two ring-opened metabolites. Also, sila-haloperidol did not form the corresponding direct glucuronidation metabolite observed for haloperidol.

Clearly, a substitution of the carbon atom in the 4-position of the piperidine ring of haloperidol by a silicon atom resulted in significant differences in the metabolic pathways of the molecule. In order to provide further support for the observed differences, the metabolism of another structurally related carbon/silicon pair was studied, namely trifluperidol and sila-trifluperidol, shown in Fig. 1. Like haloperidol, trifluperidol is a neuroleptic agent that has been used in the treatment of schizophrenia (Gallant et al., 1963). The distribution, metabolism and excretion of trifluperidol in the rat has been published previously (Souijn et al., 1966; Lewi et al., 1970). The phase I metabolism of trifluperidol and sila-trifluperidol was studied in RLMs and HLMs, whereas the phase II metabolism was studied in rat and human hepatocytes. In addition, liver microsomal incubations supplemented with UDPGA were performed. In general, both the phase I and phase II metabolism of trifluperidol/sila-trifluperidol were analogous to those of haloperidol/sila-haloperidol. The corresponding metabolites were observed for trifluperidol/sila-trifluperidol that were observed for haloperidol/sila-haloperidol, as shown in Table 4. The product ion spectra of trifluperidol and sila-trifluperidol, parent drugs and metabolites, are shown in the Supplemental data.

Discussion

Replacement of the quaternary R_3COH carbon atom of haloperidol by a silicon atom significantly altered its metabolic fate. For haloperidol, the pyridinium metabolite is formed via dehydration and oxidation of the piperidine ring to the pyridinium ion. For sila-haloperidol, the analogous sila-pyridinium ion was not formed, and new metabolic pathways originating from opening of the piperidine ring were observed.

Two pathways have been proposed for the formation of the haloperidol pyridinium metabolite. The first pathway is initiated by α-carbon (α to the nitrogen) hydroxylation followed by water elimination to yield the iminum ion that directly or via its enamine conjugate base is converted to a dihydropyridinium intermediate. The second pathway is initiated by dehydration to yield a tetrahydropyridine intermediate that then undergoes α-carbon hydroxylation to yield the dihydropyridinium intermediate. The dihydropyridinium ion is then proposed to being spontaneously oxidized to the pyridinium ion (Subramanyam et al., 1991b).

While carbon tends to form stable double and triple bonds with itself and other analogous atoms, double or triple bonds with silicon atoms are generally thermodynamically unstable under physiological conditions (Brook, 2000). The thermodynamic instability and reactivity of the Si=C double bond together with the fact that the silicon-oxygen bond is strong, explains why the silicon-oxygen bond in sila-haloperidol does not break to eliminate water and yield the Si=C bond, which is required for the formation of a sila-pyridinium metabolite.

By analogy to the pathway leading to the pyridinium metabolite of haloperidol, the metabolism of the piperidine ring of sila-haloperidol is most likely initiated by a hydroxylation at the α-carbon (α to the nitrogen), followed by a ring opening to form an

DMD Fast Forward. Published on October 7, 2009 as DOI: 10.1124/dmd.109.028449
This article has not been copyedited and formatted. The final version may differ from this version.

intermediate with an aldehyde and a secondary amine functionality. This intermediate, an α-silyl aldehyde, is very reactive and easily undergoes hydrolytic cleavage of the Si-C bond (Larson, 1996). The proposed cyclisation following the elimination of acetaldehyde is outlined in Fig. 9.

For the phase II metabolism, as revealed by the incubations with hepatocytes, the most striking difference between haloperidol and its silicon analogue is the difference in glucuronide formation. For haloperidol, the direct conjugation of the piperidine-bound hydroxyl group with glucuronic acid resulted in a significant metabolite in rat and human hepatocytes. The corresponding metabolite was not observed for sila-haloperidol.

In the rat and human microsomal incubations with UDPGA, glucuronidation was observed on the piperidine-bound hydroxyl group of haloperidol but not on the SiOH group of sila-haloperidol. A speculation would be that the direct glucuronidation of the silanol (SiOH) group occurs, but that the resulting conjugate with its hydrolytically sensitive Si-OC bond then undergoes hydrolysis to give the corresponding silanol and free glucuronic acid. In this context it is important to note that the chemical reactivity of thermodynamically very stable (but against water kinetically labile) Si-OC bond of alkoxysilanes (alkyl silyl ethers) differs significantly compared with that of the C–OC bond of analogous dialkyl ethers (Colvin, 1981; Osterholtz and Pohl, 1992). An alternative explanation for the absence of glucuronidation in the case of sila-haloperidol might be that the silanol is a poor substrate for the UDP-glucuronosyltransferases. Further studies are necessary to clarify this issue.

Decreased lipophilicity of drug molecules may be desirable since it may improve DMPK and physicochemical properties, e.g., increased solubility and decreased hepatic clearance by cytochrome P450 (Smith, 2001). A means to modify lipophilicity while retaining the major structural properties of the molecule is to introduce hydroxyl groups.

However, a common drawback of this strategy is high clearance originating from phase II metabolism, e.g., glucuronidation. Hence, if silanol (SiOH) groups do not form stable glucuronide conjugates this would provide a possibility to introduce hydrophilicity in drug molecules without allowing for direct phase II metabolism. While this is an attractive hypothesis favoring silanol analogues of drug candidates, further evaluation is needed, e.g., more structurally diverse silanol-containing compounds should be investigated. Also, if an unstable glucuronide actually is formed, studies on its potential reactivity towards biological nucleophiles must be considered.

Noteworthy is that the direct glucuronidation metabolite of trifluperidol was only formed in small amounts by human hepatocytes and not by rat hepatocytes. For haloperidol, the corresponding metabolite was observed in substantial amounts in both rat and human hepatocyte incubations. The same differences were observed in the rat and human microsomal incubations containing UDPGA. This might be explained by the fact that the chlorine atom is in the *para* position of the phenyl ring of haloperidol and the trifluoromethyl group is in the *meta* position of the phenyl ring of trifluperidol. Thus, the direct glucuronidation might occur to less extent for trifluperidol due to a larger steric hindrance from the trifluoromethyl group in the *meta* position.

Silicon analogues of known drugs might be interesting from several points of view. Replacement of a carbon atom by a silicon atom in a known drug changes the geometric and electronic properties and thereby the size, shape, conformational behaviour, chemical reactivity and lipophilicity of the molecule. This might in turn alter the interaction with a receptor and hence change the pharmacodynamics of the drug. The metabolism of the drug may change and therefore also metabolism-related toxicity. This study has shown major differences in metabolic pathways between two different pairs of carbon/silicon analogues. Another important issue is that of intellectual property; silicon analogues of known drugs

may open up for a new type of drug development process. Because the original carbon-based drug has been tested thoroughly, the corresponding silicon analogue may be able to shortcut the discovery part of drug development. Some silicon-containing drugs are currently being evaluated in clinical trials (Bains and Tacke, 2003; Gately and West, 2007), and it will be interesting to follow the outcome of those studies with respect to pharmocodynamic properties and safety compared to the original molecule.

In conclusion, structures of three major phase I metabolites of sila-haloperidol formed in human liver microsomes were proposed in a previous study (Tacke et al., 2008). The present study builds further on those data in that a comprehensive comparison between the metabolism of haloperidol and trifluperidol and their sila-analogues has been performed in several in vitro systems including liver microsomes from rats and humans with and without activation for glucuronidation, and hepatocytes from humans, rats and dogs to cover phase I as well as phase II metabolism. As a result, in addition to the three metabolites of the previous study, at least five additional phase I and phase II metabolites for each compound have been characterized and mechanisms for their formation rationalized. One major difference was the absence of the pyridinium ion metabolite, a major metabolite for haloperidol and trifluperidol, in the incubations with the silicon analogues. Instead, the piperidine ring of both silicon analogues opens metabolically, and different ring opening metabolites were observed. Another important difference was that direct glucuronidation did not occur for sila-haloperidol as it did for haloperidol. This difference was not as obvious for trifluperidol and sila-trifluperidol possibly because the trifluoromethyl group in the *meta* position may hinder direct glucuronidation for both compounds.

Acknowledgements

Dr. Binh Nguyen, University of Würzburg, is greatly acknowledged for providing a sample of sila-trifluperidol. We also thank Sara Leandersson, Petter Svanberg, Susanne Ekehed and Anna Abrahamsson for conducting the hepatocyte experiments. Prof. Neal Castagnoli Jr. is greatly acknowledged for donating synthetic metabolite reference compounds of haloperidol.

References

Bains W and Tacke R (2003) Silicon chemistry as a novel source of chemical diversity in drug design. *Curr Opin Drug Discov Dev* **6:**526-543.

Beulz-Riche D, Robert J, Menard C and Ratanasavanh D (2001) Metabolism of methoxymorpholino-doxorubicin in rat, dog and monkey liver microsomes: comparison with human microsomes. *Fundam Clin Pharmacol* **15:**373-378.

Brook MA (2000) *Silicon in Organic, Organometallic and Polymer Chemistry*. John Wiley and Sons, Inc., New York.

Casey DE (1995) Motor and mental aspects of extrapyramidal syndromes. *Int Clin Psychopharmacol* **10:**105-114.

Colvin EW (1981) Alkyl silyl ethers, in: *Silicon in Organic Synthesis*, pp 178-192, Butterworths, London.

Daiss JO, Burschka C, Mills JS, Montana JG, Showell GA, Fleming I, Gaudon C, Ivanova D, Gronemeyer H and Tacke R (2005) Synthesis, crystal structure analysis, and pharmacological characterization of disila-bexarotene, a disila-analogue of the RXR-selective retinoid agonist bexarotene. *Organometallics* **24:**3192-3199.

Daiss JO, Burschka C, Mills JS, Montana JG, Showell GA, Warneck JBH and Tacke R (2006) Sila-venlafaxine, a sila-analogue of the serotonin/noradrenaline reuptake inhibitor venlafaxine: synthesis, crystal structure analysis, and pharmacological characterization. *Organometallics* **25:**1188-1198.

Dauer W and Przedborski S (2003) Parkinson's disease: mechanisms and models. *Neuron* **39:**889-909.

Fang J, Gorrod JW, Kajbaf M, Lamb JH and Naylor S (1992) Investigation of the neuroleptic drug haloperidol and its metabolites using tandem mass spectrometry. *Int J Mass Spectrom Ion Process* **122:**121-131.

Gallant DM, Bishop MP, Timmons E and Steele CA (1963) A controlled evaluation of trifluperidol: a new potent psychopharmacologic agent. *Curr Ther Res* **5:**463-471.

Gately S and West R (2007) Novel therapeutics with enhanced biological activity generated by the strategic introduction of silicon isosteres into known drug scaffolds. *Drug Dev Res* **68:**156-163.

Gorrod JW and Fang J (1993) On the metabolism of haloperidol. *Xenobiotica* **23:**495-508.

Janssen PAJ, van de Westeringh C, Jageneau AHM, Demoen PJA, Hermans BKF, van Daele GHP, Schellekens KHL, van der Eycken CAM and Niemegeers CJE (1959) Chemistry and pharmacology of CNS depressants related to 4-(4-hydroxy-4-phenylpiperidino)butyrophenone. I. Synthesis and screening data in mice. *J Med Pharm Chem* **1:**281-297.

Larson GL (1996) The chemistry of α-silyl carbonyl compounds, in: *Advances in Silicon Chemistry* (Larson GL ed), pp 105-271, JAI Press Inc, Greenwich.

Lewi PJ, Heykants JJP and Janssen PAJ (1970) On the distribution and metabolism of neuroleptic drugs - Part III: Pharmacokinetics of trifluperidol. *Arzneim Forsch* **20:**1701-1705.

Levinson DF (1991) Pharmacologic treatment of schizophrenia. *Clin Ther* **13:**326-352.

Mills JS and Showell GA (2004) Exploitation of silicon medicinal chemistry in drug discovery. *Expert Opin Investig Drugs* **13:**1149-1157.

Miyazaki H, Matsunaga Y, Nambu K, Oh-e Y and Hashimoto M (1986) Disposition and metabolism of [^{14}C]-haloperidol in rats. *Arzneim Forsch* **36:**443-452.

Narayanan R, LeDuc B and Williams DA (2004) Glucuronidation of haloperidol by rat liver microsomes: involvement of family 2 UDP-glucuronosyltransferases. *Life Sci* **74:**2527-2539.

Nguyen BT (2009) Synthese silicumorganischer Wirkstoffe und Beiträge zur Methodenentwicklung zum Aufbau von Silazepan- und Silapyrrolidin-Derivaten., University of Würzburg, Würzburg, Germany.

Oida T, Terauchi Y, Yoshida K, Kagemoto A and Sekine Y (1989) Use of antisera in the isolation of human specific conjugates of haloperidol. *Xenobiotica* **19:**781-793.

Osterholtz FD and Pohl ER (1992) Kinetics of the hydrolysis and condensation of organofunctional alkoxysilanes: a review. *J Adhesion Sci Technol* **6:**127-149.

Pooni PK and Showell GA (2006) Silicon switches of marketed drugs. *Mini Rev Med Chem* **6:**1169-1177.

Popp F (2008) 2,4,6,-Trimethyoxyphenylsilane: Verwendung als geschützte Bausteine für die Synthese silicumhaltiger Wirkstoffe sowie als Silylierungreagenzien., University of Würzburg, Würzburg, Germany.

Ramanathan R, Su AD, Alvarez N, Blumenkrantz N, Chowdhury SK, Alton K and Patrick J (2000) Liquid chromatography/mass spectrometry methods for distinguishing N-Oxides from hydroxylated compounds. *Anal Chem* **72:**1352-1359.

Showell GA and Mills JS (2003) Chemistry challenges in lead optimization: silicon isosteres in drug discovery. *Drug Discovery Today* **8:**551-556.

Smith DA (2001) The long, hard road: drug metabolism in the lifetime of the DMDG. *Xenobiotica* **31:**459 - 467.

Someya T, Shibasaki M, Noguchi T, Takahashi S and Inaba T (1992) Haloperidol metabolism in psychiatric patients: importance of glucuronidation and carbonyl reduction. *J Clin Psychopharmacol* **12:**169-174.

Souijn W, van Wijngaarden I and Allewijn F (1966) Distribution, excretion and metabolism of the neuroleptics of the butyrophenone type. *Eur J Pharmacol* **1:**47-57.

Subramanyam B, Pond SM, Eyles DW, Whiteford HA, Fouda HG and Castagnoli Jr N (1991a) Identification of potentially neurotoxic pyridinium metabolite in the urine of schizophrenic patients treated with haloperidol. *Biochem Biophys Res Commun* **181:**573-578.

Subramanyam B, Woolf T and Castagnoli Jr N (1991b) Studies on the in vitro conversion of haloperidol to a potentially neurotoxic pyridinium metabolite. *Chem Res Toxicol* **4:**123-128.

Tacke R, Heinrich T, Bertermann R, Burschka C, Hamacher A and Kassack MU (2004a) Sila-haloperidol: A silicon analogue of the dopamine (D_2) receptor antagonist haloperidol. *Organometallics* **23:**4468-4477.

Tacke R and Linoh H (1989) Bioorganosilicon chemistry, in: *The chemistry of organic silicon compounds* (Patai S and Rappoport Z eds), John Wiley & Sons Ltd, Chichester.

Tacke R, Popp F, Müller B, Theis B, Burschka C, Hamacher A, Kassack MU, Schepmann D, Wünsch B, Jurva U and Wellner E (2008) Sila-haloperidol, a silicon analogue of the dopamine ($D_{2)}$ receptor antagonist haloperidol: synthesis, pharmacological properties, and metabolic fate. *ChemMedChem* **3:**152-164.

Tacke R, Schmid T, Penka M, Burschka C, Bains W and Warneck J (2004b) Syntheses and pharmacological properties of the histaminic H_1 antagonists sila-terfenadine-A, sila-terfenadine-B, disila-terfenadine, and sila-fexofenadine: A study on C/Si bioisosterism. *Organometallics* **23:**4915-4923.

Legends for figures

Fig. 1 Structures of the test compounds.

Fig. 2. Proposed overall metabolism of haloperidol in HLMs, RLMs and hepatocytes (HH - human, DH - dog, RH - rat).

Fig. 3. Proposed overall metabolism of sila-haloperidol in HLMs, RLMs and hepatocytes (HH - human, DH - dog, RH - rat).

Fig. 4. Product ion spectrum of sila-haloperidol.

Fig. 5. Proposed fragmentation pathways of sila-haloperidol.

Fig. 6. The product ion spectrum of the ring-opened metabolite1 of sila-haloperidol.

Fig. 7. Proposed fragmentation pathways of the ring-opened metabolite1 of sila-haloperidol.

Fig. 8. Metabolism of haloperidol and sila-haloperidol, respectively, by human hepatocytes. Extracted ion chromatograms of *m/z* 212, 552, 378, 392 and 354 for haloperidol, and *m/z* 228, 364, 382 and 394 for sila-haloperidol. The retention times of haloperidol and sila-haloperidol are marked in the different chromatograms.

Fig. 9. Proposed mechanism for the metabolic ring opening of sila-haloperidol.

DMD Fast Forward. Published on October 7, 2009 as DOI: 10.1124/dmd.109.028449
This article has not been copyedited and formatted. The final version may differ from this version.

TABLE 1

Relative metabolite amounts of the fraction metabolized of haloperidol. Liver microsomes incubated for 60 min and hepatocytes incubated for 120 min. Data estimated from integration of extracted ion chromatograms.

			Haloperidol				
Metabolite	*m/z*	t_R (min)	RLM	HLM	rat heps	dog heps	human heps
Relative proportions of metabolites after incubation of haloperidol for 60/120 min (%)							
N-dealk	212	1.06	7	9	32	37	5
+OH+Gluc	568	1.43	N.D.	N.D.	2	0	0
Gluc	552	1.62	N.D.	N.D.	10	0	17
OH1	392	1.71	3	2	1	0	0
OH2	392	1.78	3	1	1	0	0
Red	378	1.84	9	2	12	40	46
N-oxide1	392	2.08	1	1	1	0	1
Pyridinium	354	2.18	73	83	39	14	31
N-oxide2	392	2.23	4	1	4	9	0
Fraction of parent drug remaining after incubation (%)							
Haloperidol	376	1.97	55	59	77	81	86

N.D., not determined (no addition of UDPGA in this experiment)

DMD Fast Forward. Published on October 7, 2009 as DOI: 10.1124/dmd.109.028449
This article has not been copyedited and formatted. The final version may differ from this version.

TABLE 2

Relative metabolite amounts of the fraction metabolized of sila-haloperidol. Liver microsomes incubated for 60 min and hepatocytes incubated for 120 min. Data estimated from integration of extracted ion chromatograms.

Sila-haloperidol

Metabolite	*m/z*	t_R (min)	RLM	HLM	rat heps	dog heps	human heps
Relative proportions of metabolites after incubation of sila-haloperidol for 60/120 min (%)							
N-dealk	228	1.22	21	11	44	5	12
Ring-opened1+OH	380	1.28	2	2	0	0	0
+OH+Gluc	584	1.52	N.D.	N.D.	39	0	0
Ring-opened1	364	1.74	4	63	0	10	25
+OH+Sulfate	488	1.82	N.D.	N.D.	3	0	0
OH	408	1.90	71	3	5	0	0
Ring-opened2	382	1.94	1	20	0	2	7
Red	394	2.01	1	1	9	84	56
Fraction of parent drug remaining after incubation (%)							
Sila-haloperidol	392	2.18	83	65	80	61	94

N.D., not determined (no addition of UDPGA in this experiment)

DMD Fast Forward. Published on October 7, 2009 as DOI: 10.1124/dmd.109.028449
This article has not been copyedited and formatted. The final version may differ from this version.

TABLE 3

Sila-haloperidol and metabolites – fragmentation ions

Metabolite	t_R (min)	$[M+H]^+$ *m/z*	major product ions *m/z*
N-dealk	1.22	228.0608	190.0103, 192.0023, 172.0007, 173.9888
Ring-opened1+OH	1.28	380.0875	380.0869, 382.0974, 188.9782, 190.9616, 164.0897
+OH+Gluc	1.52	564.1508	584.1495, 586.1488, 408.1197, 410.1167, 165.0723, 164.0868
Ring-opened1	1.74	364.0931	364.0929, 366.0962, 172.9830, 174.9805, 164.0888
+OH+Sulfate	1.82	488.0763	408.1190, 165.0749, 164.0860, 123.0249
OH	1.90	408.1191	408.1189, 410.1153, 165.0714, 164.0877, 123.0277
Ring-opened2	1.94	382.1031	382.0978, 172.9830, 174.9806, 165.0711, 164.0943, 123.0249
Red	2.01	394.1405	394.1395, 396.1375, 376.1292, 378.1279, 320.0648, 322.0673, 172.9824, 174.9797, 109.0477
Sila-haloperidol	2.18	392.1238	392.1243, 394.1137, 165.0698, 164.0886, 123.0283

DMD Fast Forward. Published on October 7, 2009 as DOI: 10.1124/dmd.109.028449
This article has not been copyedited and formatted. The final version may differ from this version.

TABLE 4

Relative metabolite amounts of the fraction metabolized of trifluperidol and sila-trifluperidol, respectively. Liver microsomes incubated for 60 min and hepatocytes incubated for 120 min. Data estimated from integration of extracted ion chromatograms.

Trifluperidol

Metabolite	*m/z*	t_R (min)	RLM	HLM	rat heps	human heps
Relative proportions of metabolites after incubation of trifluperidol for 60/120 min (%)						
N-dealk	246	1.19	42	35	51	30
+OH+Gluc	602	1.58	N.D.	N.D.	1	0
Gluc	586	1.65	N.D.	N.D.	0	1
OH1	426	1.81	3	<1	0	0
OH2	426	1.86	3	2	1	1
Red	412	1.90	8	1	12	12
N-oxide1	426	2.10	<1	1	<1	1
Pyridinium	388	2.17	43	60	35	55
N-oxide2	426	2.23	1	1	<1	1
Fraction of parent drug remaining after incubation (%)						
Trifluperidol	410	2.03	59	34	50	67

Sila-trifluperidol

Metabolite	*m/z*	t_R (min)	RLM	HLM	rat heps	human heps
Relative proportions of metabolites after incubation of sila-trifluperidol for 60/120 min (%)						
N-dealk	262	1.32	55	40	34	41
Ring-opened1+OH	414	1.59	15	0	0	0
+OH+Gluc	618	1.65	N.D.	N.D.	60	0
Ring-opened1	398	1.80	9	46	0	37

Ring-opened2	416	1.98	3	13	0	13
OH	442	2.01	18	1	6	0
Red	428	2.03	0	0	0	8
Fraction of parent drug remaining after incubation (%)						
Sila-trifluperidol	426	2.18	21	62	56	79

N.D., not determined (no addition of UDPGA in this experiment)

Figure 1.

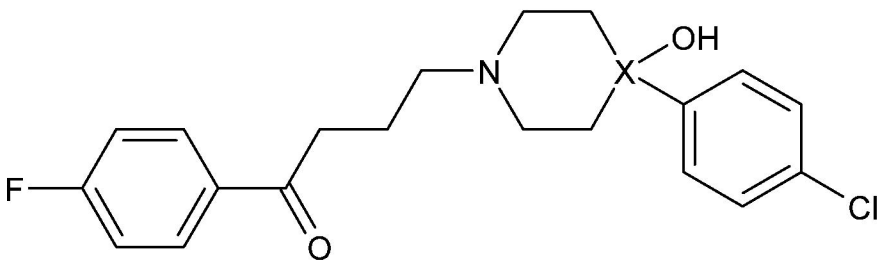

X = C: Haloperidol
X = Si: Sila-haloperidol

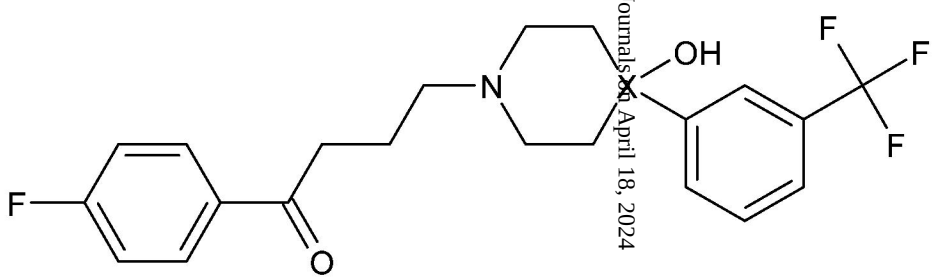

X = C: Trifluperidol
X = Si: Sila-trifluperidol

Figure 2.

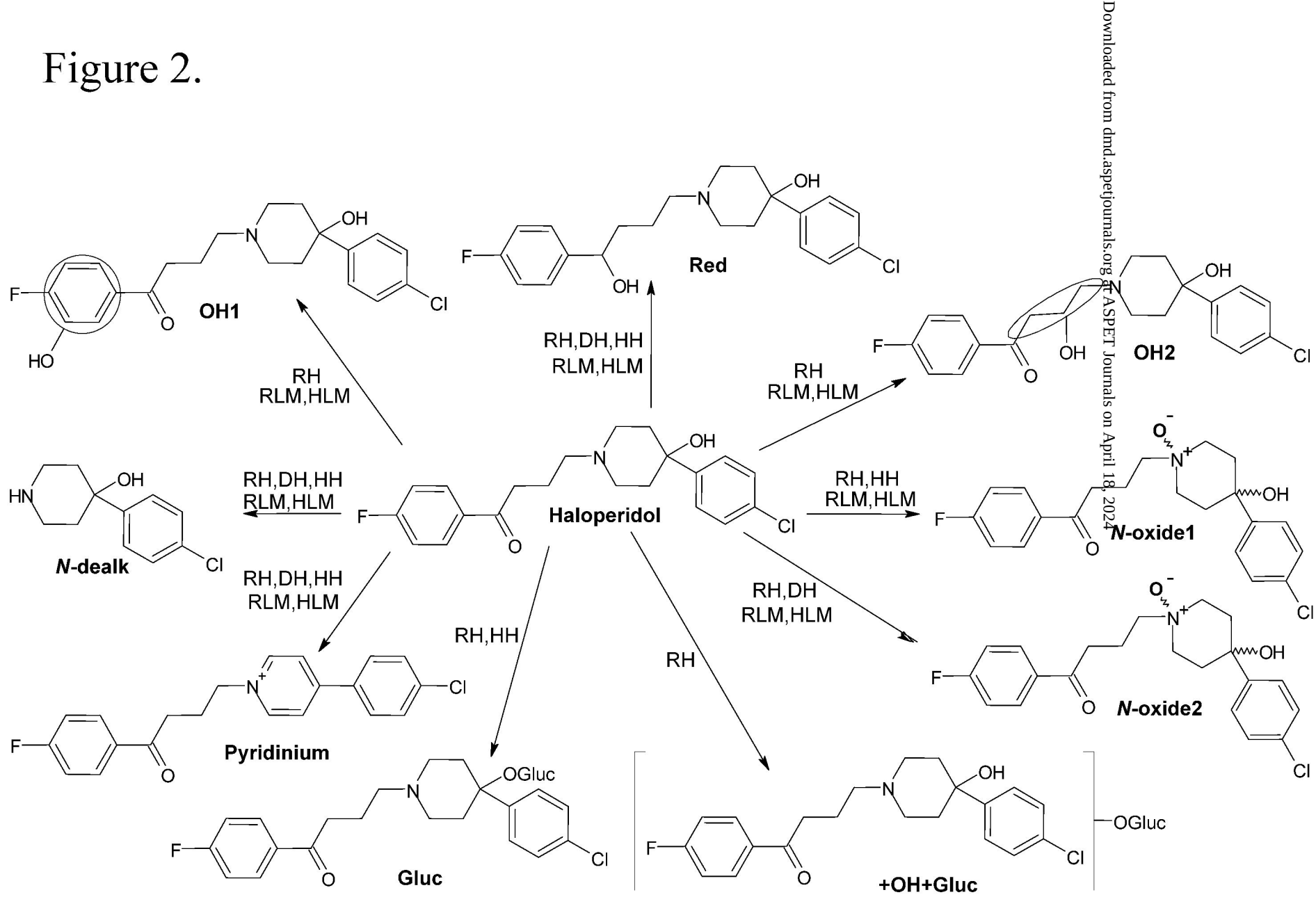

Figure 3.

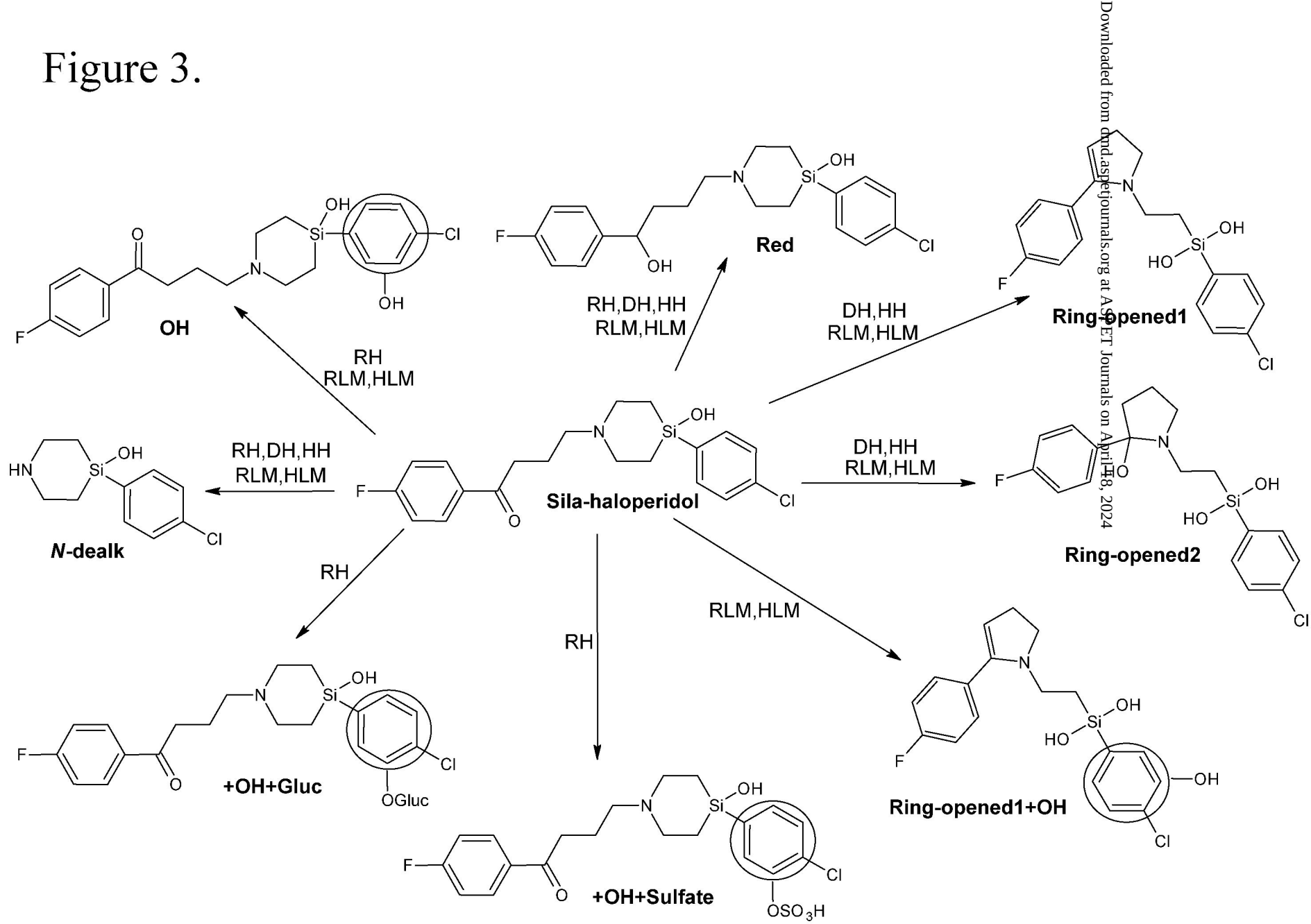

Figure 4.

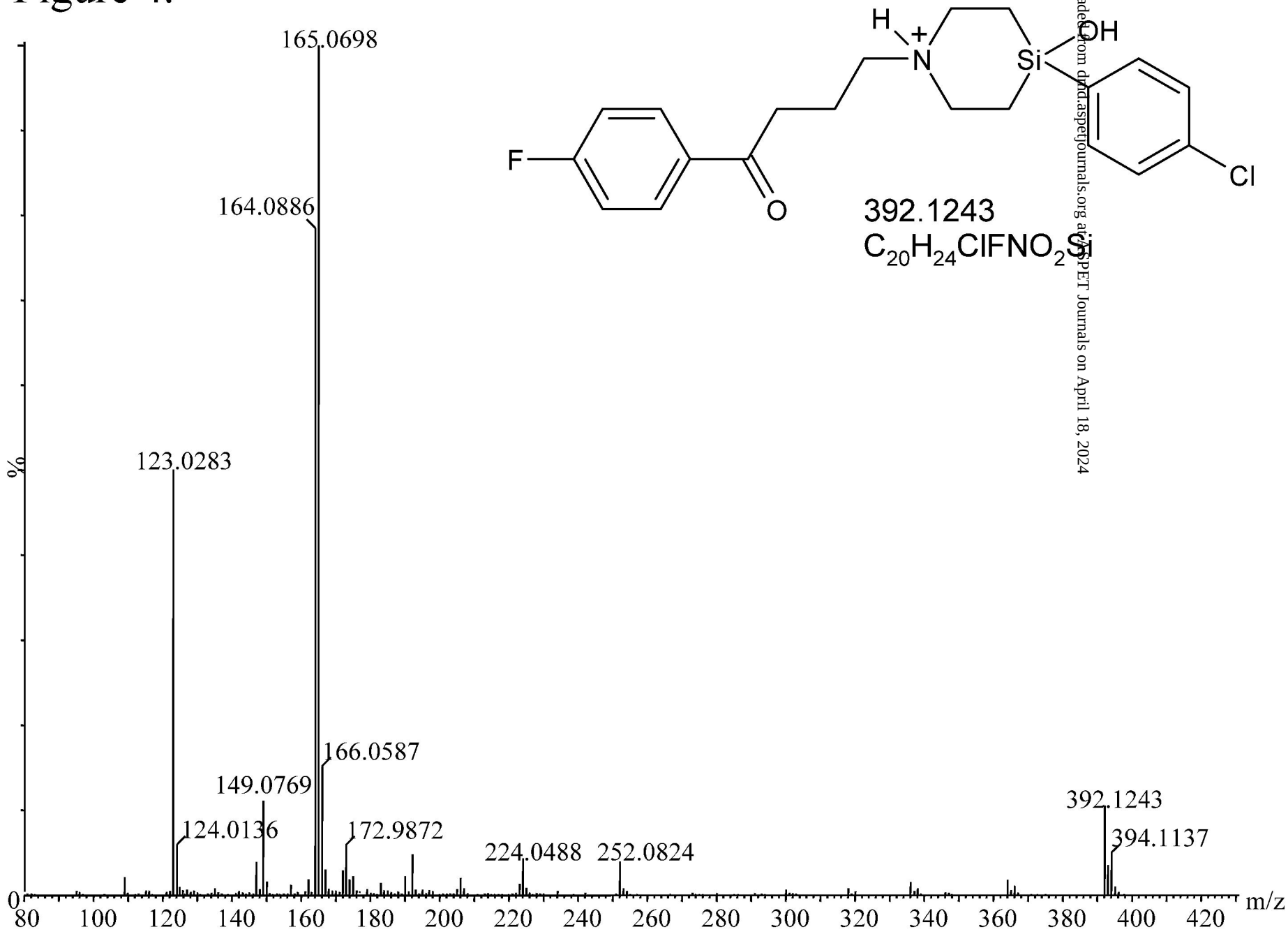

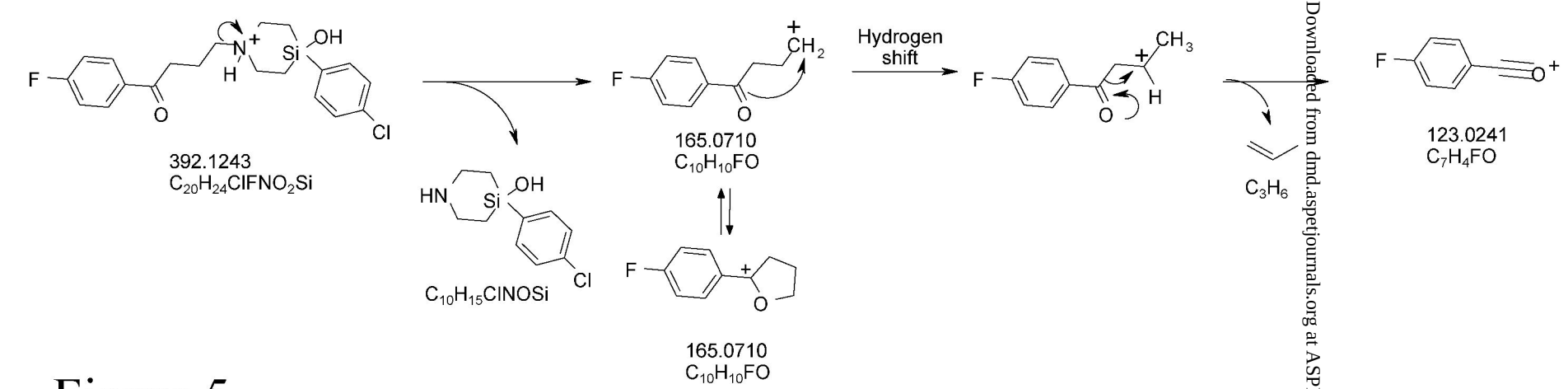

Figure 5.

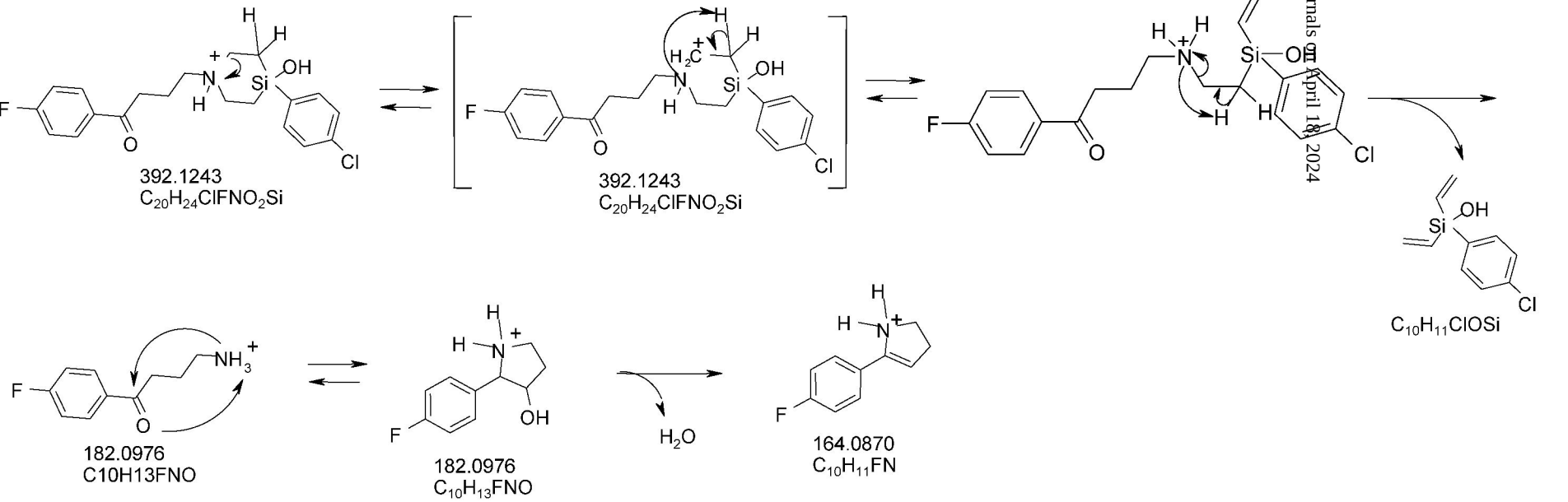

Figure 6.

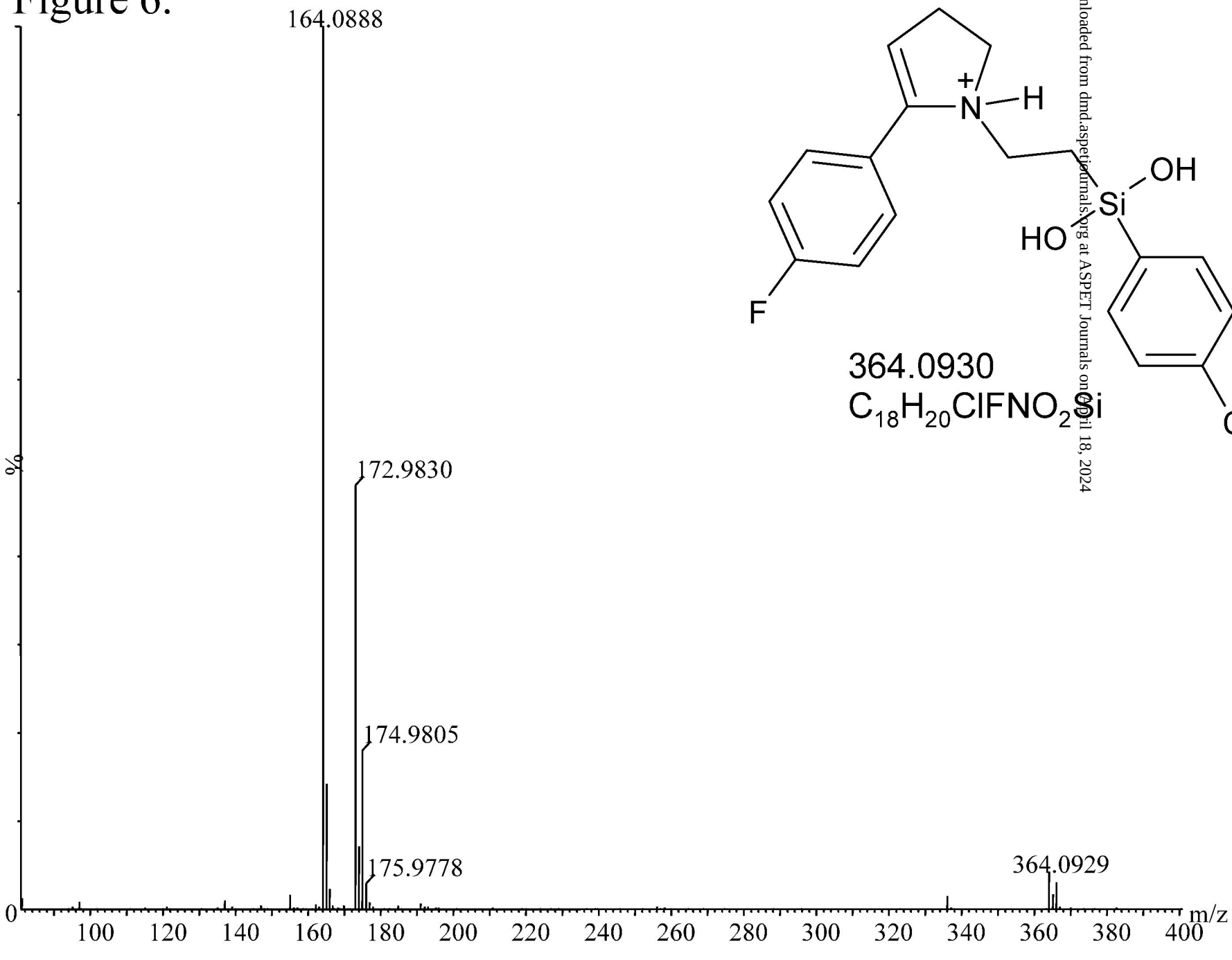

Figure 7.

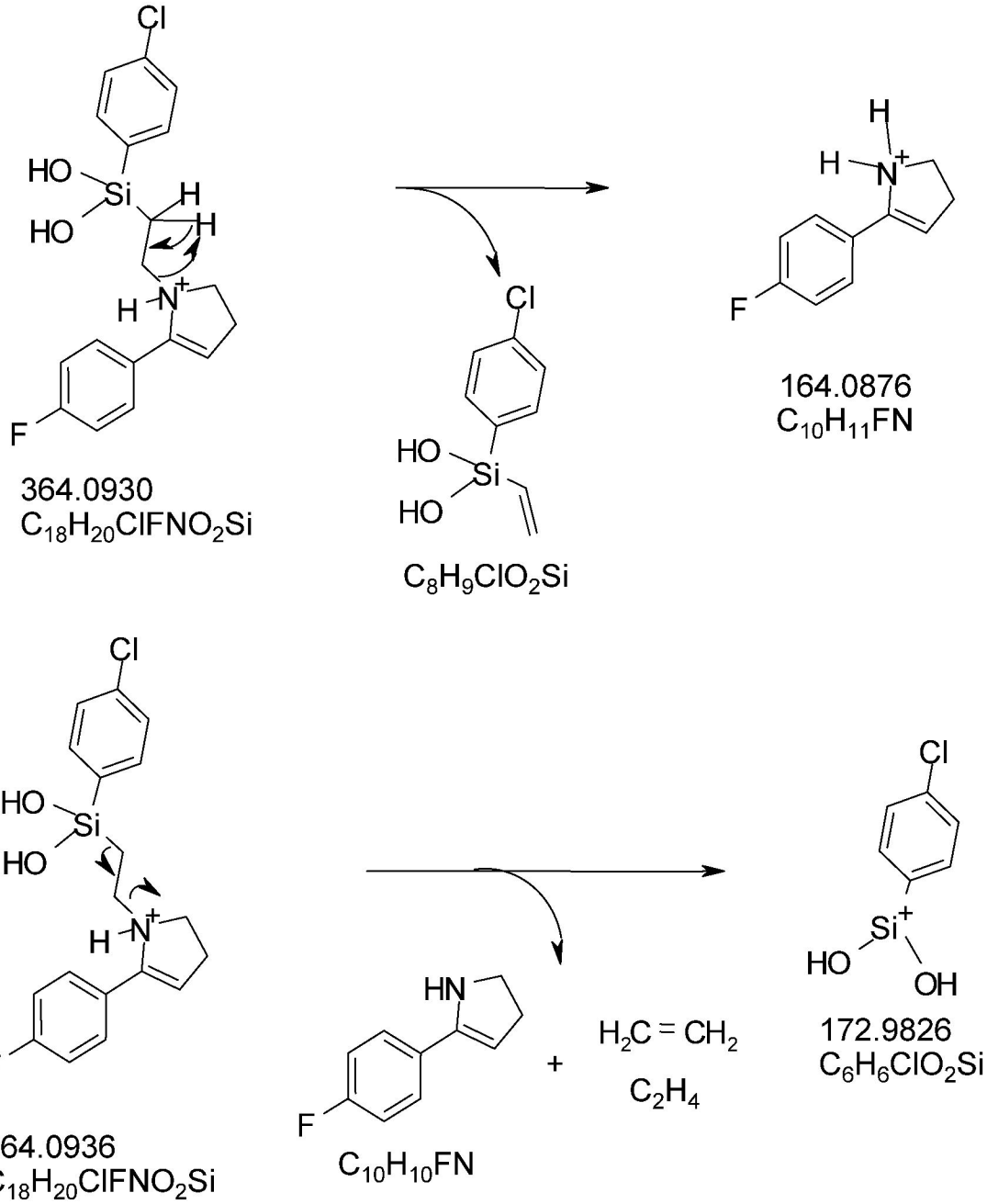

Figure 8.

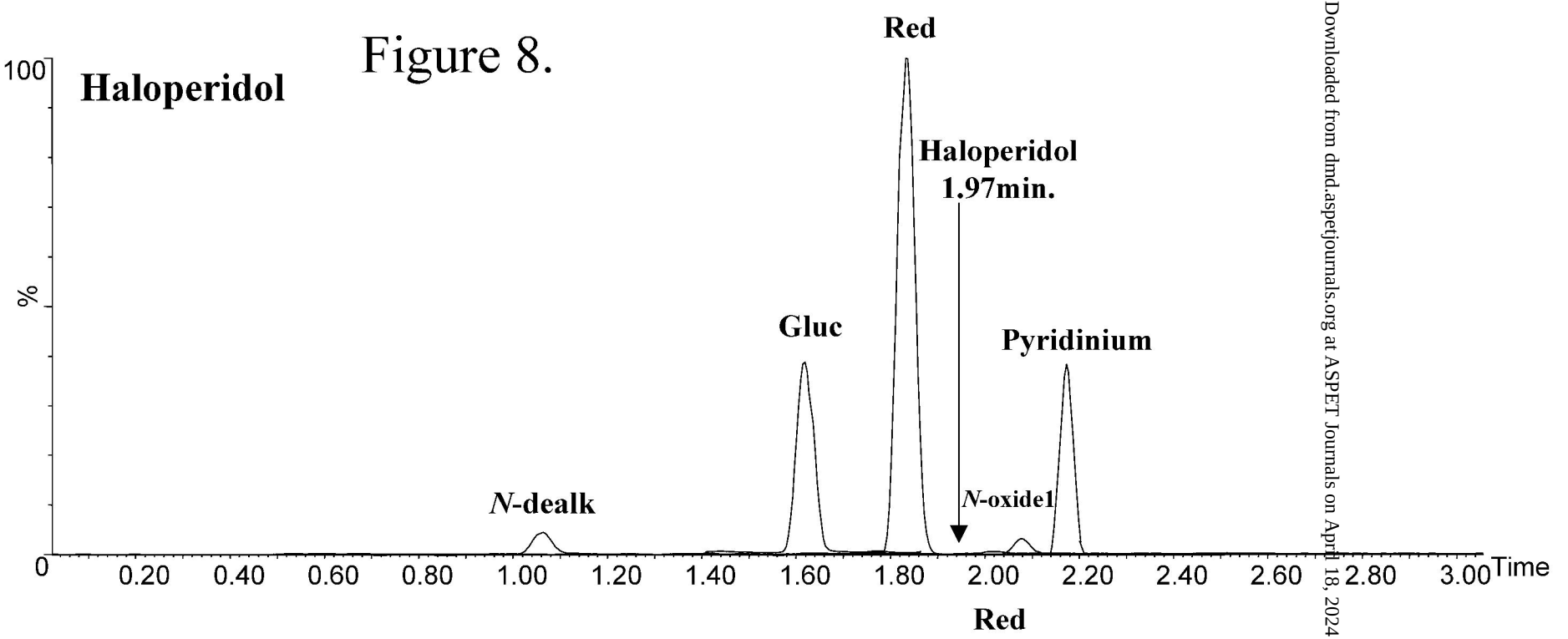

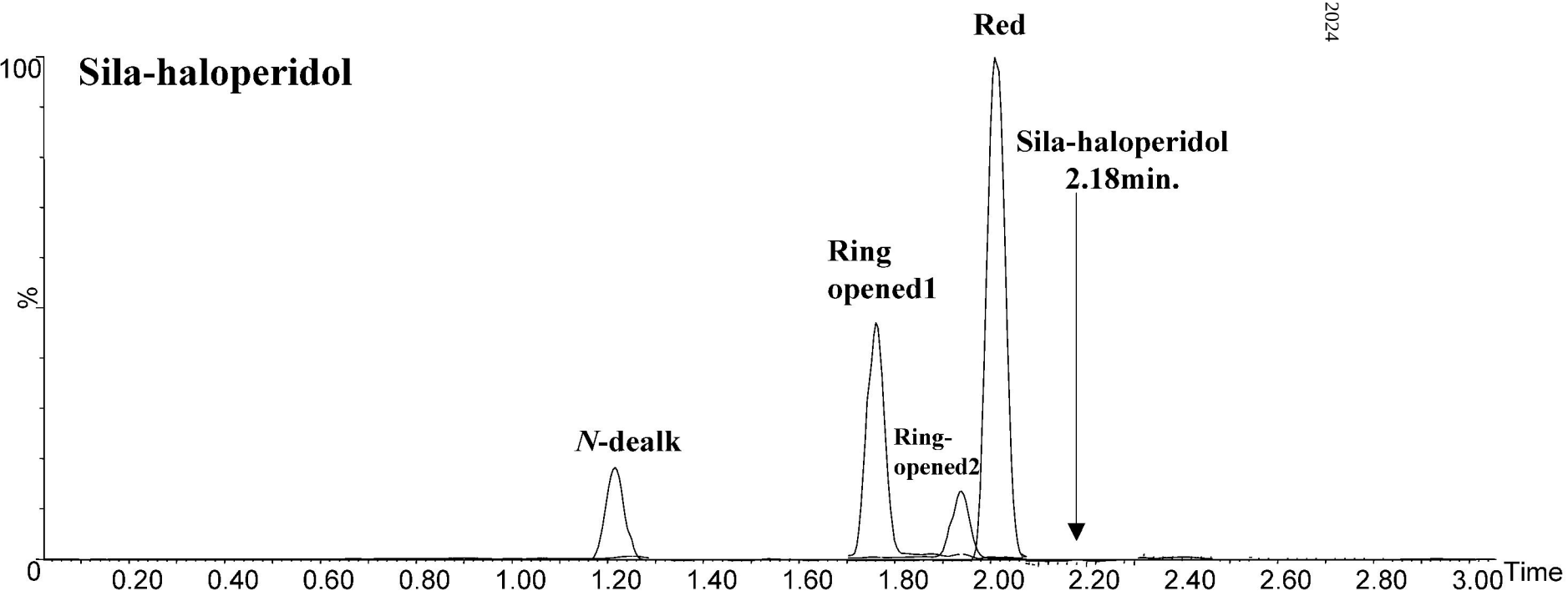

Figure 9.